OpenNano 8 (2022) 100093

Contents lists available at ScienceDirect

OpenNano

journal homepage: www.elsevier.com/locate/onano

Full length article

Successive cytotoxicity control by evolutionary surface decorated electronic push-pull green ZnCr-LDH nanostructures: Drug delivery enlargement for targeted breast cancer chemotherapy

Mahsa Kiani [a], Mojtaba Bagherzadeh [a,*], Yousef Fatahi [b,c], Hossein Daneshgar [a], Moein Safarkhani [a], Ghazal Salehi [a], Pooyan Makvandi [d], Mohammad Reza Saeb [e], Eder C. Lima [f], Navid Rabiee [g,h,*]

[a] Department of Chemistry, Sharif University of Technology, Tehran, Iran
[b] Department of Pharmaceutical Nanotechnology, Faculty of Pharmacy, Tehran University of Medical Sciences, Tehran 14155-6451, Iran
[c] Nanotechnology Research Centre, Faculty of Pharmacy, Tehran University of Medical Sciences, Tehran 14155-6451, Iran
[d] Istituto Italiano di Tecnologia, Centre for Materials Interfaces, viale Rinaldo Piaggio 34, Pontedera, Pisa 56025, Italy
[e] Department of Polymer Technology, Faculty of Chemistry, Gdańsk University of Technology, G. Narutowicza 11/12 80-233, Gdańsk, Poland
[f] Institute of Chemistry, Federal University of Rio Grande Do Sul (UFRGS), Av. Bento Goncalves 9500, Postal Box, 15003, ZIP, 91501-970, Brazil
[g] School of Engineering, Macquarie University, Sydney, New South Wales 2109, Australia
[h] Department of Materials Science and Engineering, Pohang University of Science and Technology (POSTECH), 77 Cheongam-ro, Nam-gu, Pohang, Gyeongbuk 37673, South Korea

ARTICLE INFO

Keywords:
LDH
Cytotoxicity
Leaf extract
Benzamides
In vitro
In vivo

ABSTRACT

The reason for the increasing bioavailability and biocompatibility of the porous nanomaterials in the presence of different (bio)molecules is still unknown. The role of difference functional groups and their interactions with the potential bioavailability and biocompatibility is of great importance. To investigate the potential contribution of the electronic effects (especially on the surface of the porous nanomaterials) on their biomedical behavior, a series of surface-decorated green ZnCr-layered double hydroxide (LDH) porous nanocarriers is developed as a non-viral vector. Different conjugations investigated these porous LDHs for optimizing and minimizing the cytotoxicity for targeted breast cancer therapy. Quick low-temperature synthesized ZnCr-LDH nanocarriers method with enlarged drug delivery windows decorated with leaf extracts and benzamide-like molecules revealed a push-pull electronic synergistic effect on cytotoxicity and enhanced cell viability, biocompatibility, aggregations, and interactions with the cell membranes. The pre-defined model drug, doxorubicin (DOX), unraveled chemotherapy performance in response to MCF-7 cell lines, with ≈ 60% drug payload contributed from functional groups of leaf extracts. Moreover, electron-poor and electron-rich benzamide-like molecules attached to the ZnCr-LDH surface enhanced the relative cell viability up to 29% and 32%, respectively. The *in vivo* experiments on breast cancer of treated mice (H&E) revealed unaggregated cellular arrays and antibacterial activity against *E. coli* (gram-negative) and *S. aureus* (gram-positive) bacteria. Benzamide-like ZnCr-LDH nanocarriers showed a suitable zone of inhibition beyond 10 mm, compared to the standard. Cytotoxicity control achieved herein seems promising for the future ahead of nanomedicine.

* Corresponding authors.
E-mail addresses: bagherzadeh@sharif.edu (M. Bagherzadeh), nrabiee94@gmail.com (N. Rabiee).

https://doi.org/10.1016/j.onano.2022.100093
Received 5 September 2022; Received in revised form 3 October 2022; Accepted 11 October 2022
Available online 12 October 2022

1. Introduction

Numerous studies have been carried out on different nanoparticles for multiple applications, but green and cost-effective approaches still lure the attention of nano-scale scientists [1,2]. Porous and platelet-like nano-scale particles can physically and/or chemically interact with contaminants, drugs, and cells. Over the last two decades, layered double hydroxides (LDHs) have shown exceptional ability to establish both physical and chemical bonds with different materials [3,4], particularly in interactions with various biomolecules [5]. In a series of previous studies on a wide range of porous nanomaterials, including metal-organic frameworks (MOFs) and LDHs, it was shown that the surface functionalization of those porous nanomaterials with different molecules and/or natural components considerably affects their interaction selectivity [6]. All of these targeted interactions could lead to different applications; for instance, by covering the LDHs surface with leaf extracts of *Rosmarinus officinalis*, the relative cell viability is augmented, and the antibacterial activity of the LDHs improved [7].

From another perspective, by the layer-by-layer decoration of fluorescent active proteins and surface modifications of the porphyrins of the LDHs, their sensitivity towards the use in the application of CRISPR-delivery increased [6]. This ability is related to the functional groups attached to the surface, the nature of the precursors used, and the unreacted compounds/components present on the surface [8]. Our previous works on uncontrolled surface modification studies (uncontrolled due to the non-selected pattern modifications) showed that using any type of small biocompatible molecules could alter the electronic push-pull effects on the surface concerning the interactions with the cellular membranes [9]. Moreover, these interactions even can accelerate/improve the cellular internalizations in a system with no potential, like our previous report on using a rigid porphyrin structure to improve the catalytic internalization process on the interface between the MOF and cells [10].

Another thing that should be addressed is to gain a cost-effective product. To this aim, we started a series of works investigating the potential applications of unpurified porous (nano)materials [11]. Our results showed that, by using unpurified porous (nano)materials, the interactions on the interface of the (nano)material increased substantially, but the cytotoxicity did not present a significant negative impact. Therefore, not providing a complete purification before using for the co-delivery applications [12] and/or (bio) sensory applications [13] is not considered a negative point anymore.

One important question, till now, has been hidden from the scientific communities. What are the interrelationships between different electronic effects on the surface of the porous nanomaterials, including LDHs, with their biomedical behavior? The term "biomedical behavior" could be considered for cytotoxicity, biocompatibility, (bio)catalytic processes on the surface of the cells/tissues, reaction oxygen species (ROS) generation abilities, cellular internalization, folding of the genetic materials, and so many other bio-inspired/physiological mechanisms involved.

Some of the research groups checked the photophysical properties of different push-pull electronic effects on the surface of porous nanomaterials, including LDHs, which led to the flourishing of advanced pure science to design highly efficient photo-induced devices/techniques [14,15]. The results lead to the conclusion of using more electron-donating small molecules on the surface for photophysical applications and using more linear molecules without the benzene-based groups on their backbone for the photo-(photo) catalytic applications [16,17]. However, most of their results depend on the used environment like pH, solvent, temperature, *in vitro* or ex vivo conditions, etc.; therefore, it is highly suggested to investigate each biomedical behavior with a pattern of different molecules. These patterns of molecules should have electron-donating, electron-withdrawing, resonance-rich, resonance-poor, and different functional groups in their chemical structures.

Limited experiments explore the abilities of different push-pull electronic effects on the biomedical sciences. Some preliminary results in the literature [18] emphasize the single molecules and their roles in the biomedical sciences. However, there is no report regarding the role of electron-withdrawing and electron-donating ligands/linkers on the surface of the inorganic nanomaterials, including LDHs. This is important because of bio-electro-catalytic responses and/or mechanisms in every physiological system, including the human body. Moreover, those responses and/or mechanisms are involved in the progression and advancement of abnormal structures/cells, including cancers as well. Therefore, investigating the role of different surface-functionalized molecules, especially benzamide-like molecules, due to their antidiabetic properties, on the relative cell viability, antibacterial activity, interactions at the cellular level, and drug internalizations is essential.

If we want to investigate the potential relationships between the porous LDH modified with benzamide-like molecules (with different electronic properties) and their biomedical behavior, it is important to consider a highly possible toxic and low-promising LDH. Therefore, we could be able to observe the changes in cytotoxicity clearly, and also observe the improvements in biomedical performances easily. For this aim, ZnCr LDH was chosen because the literature revealed the low possibility of using this kind of LDH for drug delivery applications [19].

Therefore, by the surface decoration of ZnCr LDH, with the leaf extracts and conjugation of those extracts to different benzamide-like molecules, a pattern may be generated from different perspectives based on their electronic properties. In this work, the aim is to investigate the role of different types of benzamide-like molecules decorated on the surface of the ZnCr LDH, on their antibacterial, drug delivery, drug loading and release behavior. Also, their possible differences in the surface morphology, with the aim to connect these results to their biomedical performances was studied.

2. Experimental

2.1. Materials and methods

Plantago major leaves were collected from Iran. The LDH used in this work is prepared by the hydrothermal method. $Zn(NO_3)$ and $Cr(NO_3)_2$ from Aldrich and sodium hydroxide from Fluka were used in this work (Scheme 1). The samples were characterized by FTIR, PXRD, AFM, and FESEM. In addition, FT-IR spectra were recorded at room temperature in the 400–4000 cm^{-1} in KBr pellets by JASCO FT-IR-460 spectrometer in the 400–4000 cm^{-1}. X-ray diffraction (XRD) spectra were acquired using an X-ray diffractometer (Philips X'Pert) with Cu Ka radiation (30 mA and 40 kV and) for 2θ values over 10–80° Field-emission scanning electron microscopy (TESCAN MIRA-3) under an acceleration voltage of 30–250 kV was utilized to characterize the nanoparticles.

2.2. Synthesis 1–5 ligands

The general procedure of the synthesis of 4-aminobenzohydrazide, 4-(2-(4-(3-carboxypropanamido)benzoyl)hydrazineyl)−4-oxobutanoic acid, 4-fluoro-N-(4-(2-(4-fluorobenzoyl)hydrazine-1-carbonyl)phenyl)benzamide, 4-methoxy-N-(4-(2-(4-methoxybenzoyl)hydrazine-1-carbonyl)phenyl)benzamide, 4-nitro-N-(4-(2-(4-nitrobenzoyl)hydrazine-1-carbonyl)phenyl)benzamide and N-(4-(2-(phenylsulfonyl)hydrazine-1-carbonyl)phenyl)benzenesulfonamide was conducted based on our previous works [9].

2.3. Synthesis of ZnCr LDH

The hydrothermal method was used to synthesize ZnCr LDH (Scheme 1). For the synthesis of solution A, a 2:1 molar ratio of Zn (NO_3) and $Cr(NO_3)_2$ in 50 mL of deionized water was made. Solution B contains 0.5 M sodium hydroxide, which is added drop by drop to solution A to reach a pH of 9–10. Finally, transferred the solution to an autoclave 100 mL and placed in an oven at 120 °C for 24 h. After this period, the solution is cooled and centrifuged, and the resulting precipitate is dried in an oven at 70 °C after several washed with deionized water and ethanol. Atomic force microscopy (AFM) observations were performed on DI nanoscope IV using a tapping mode.

2.4. Preparation of Plantago major (B) extract

After purchasing *Plantago major*, the leaves were washed with distilled water and dried at room temperature. After drying with a grinder, it was powdered to get a better extract. The finely *Plantago major* was dispersed with 200 ml of deionized water at 80 °C for 1 hour, and after this time, the mixture was cooled and filtered through, and the extract and subsequently stored at 3 °C.

2.5. Preparation of ZnCr/B

In order to decorate the extract on the surface of ZnCr LDH, 10 ml of *Plantago major* extract with 1 g of ZnCr LDH is stirred at room temperature for 10 h; then, the mixture is centrifuged and dried in an oven at 80 °C.

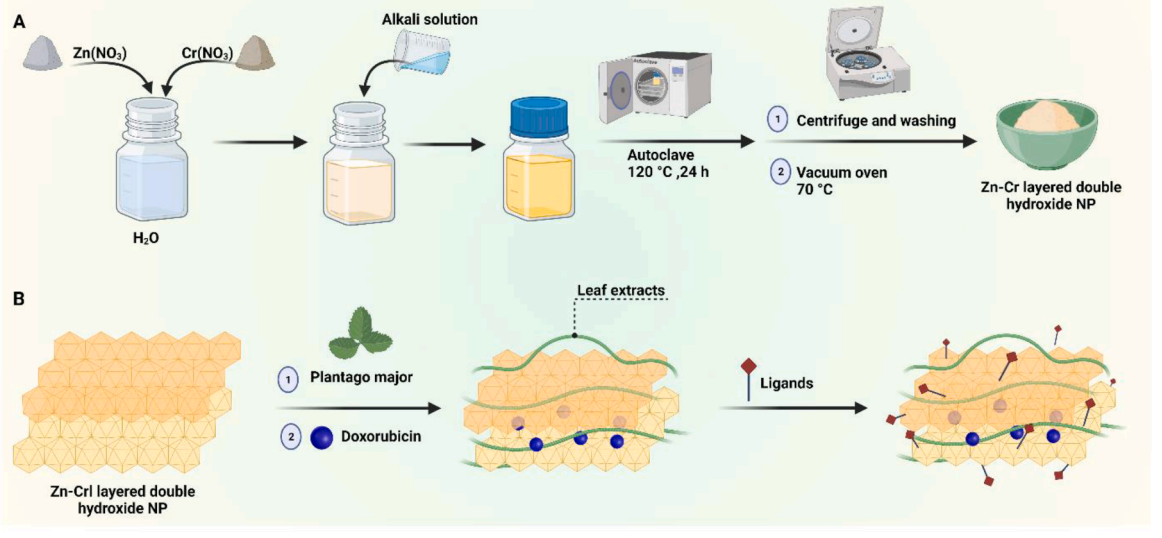

Scheme 1. Schematic illustration for fabrication of Zn-Cr layered double hydroxide nanoparticles (A) and its nanocomposites (B).

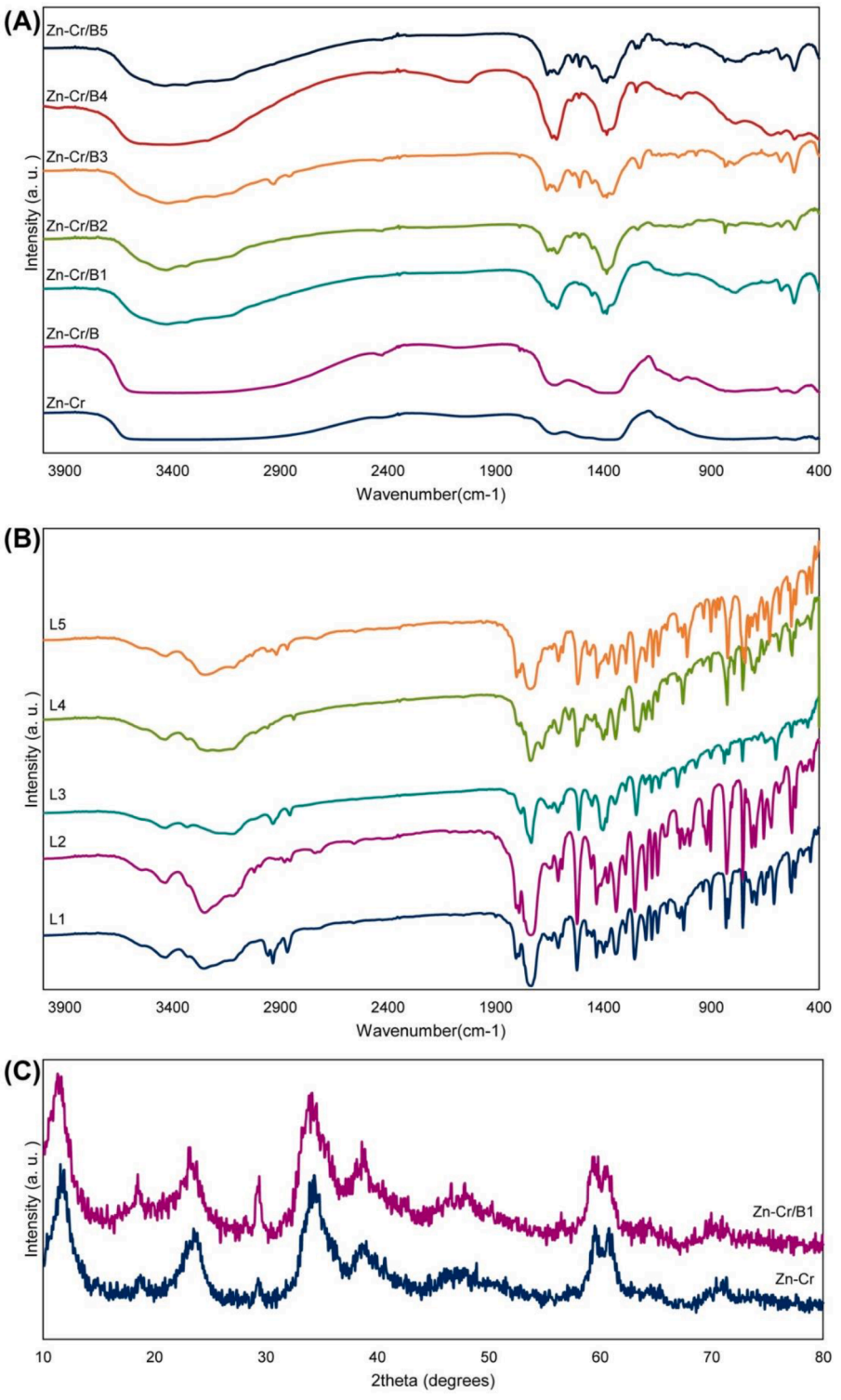

Fig. 1. FTIR spectra of the nanocomposites and ZnCr LDH (A), the benzamide-like small molecules (B); and the XRD pattern of the ZnCr LDH and ZnCr LDH@B1.

2.6. Preparation of $ZnCr/B_{1-5}$ nanocomposite

Briefly, for synthesizing the final nanocomposite with ligands 1 to 5, a solution containing 0.2 g of each ligand with a molar ratio of 1:1 of water and ethanol was made separately. Next step, 1 g of ZnCr/B precipitate was added to a solution of ligand and stirred at room temperature for 24 h, the reaction mixture was filtered, and the precipitate was dried in an oven at 80 °C.

2.7. Antibacterial activity

The synthesized nanocomposites and ligands were used separately for antibacterial testing. *Escherichia coli* was used as a gram-negative bacterium, and *Staphylococcus aureus* was used as a gram-positive bacterium. Based on the literature, the disk diffusion method was used to perform this test [20]. In this way, different concentrations were made from all the compounds, and finally, the optimal concentration of 20 μg/ml was selected. The minimum zone of inhibition (MZI) is the diameter of the killing of bacteria by the complexes, which is reported in millimeters. Also, all solutions are prepared in an aqueous solvent. Therefore, MZI produced by complexes *versus* antibiotic standards at the same concentrations is reported. The antibacterial activity of the ligands has also been investigated, but no activity has been shown. Also, water, as a negative control, has no antibacterial activity.

2.8. Cell viability assay

The cells were grown in DMEM high glucose supplemented with 1% penicillin-streptomycin and 10% fetal bovine serum and incubated at moist temperature with 5% CO_2 at 37°C. Cell viability was determined by MTT (3-(4,5 dimethylthiazol-2yl)−2,5-dihenyl-tetrazolium bromide) assay to investigate the cytotoxic effect of the synthesized nanomaterials. Briefly, the HEK-293, HT-29, and MCF-7 cell lines (1×10^5 cells/well) were seeded separately in 96-well plates. After 24 h, the culture medium was replaced with different concentrations of the nanomaterials and incubated for another 24 h. Then, the cells were washed with PBS, and 20 μL of MTT solution (6.4 mg/mL in PBS) was added to all of the wells, followed by incubation of the plate at 37 °C for 4 h. Finally, 100 μL of DMSO was added to all of the wells and shaken for 15 min. Then, the absorbance was read at 570 nm by an ELIZA reader (BioRad, CA). IC50 values were determined using an MTT assay.

2.9. In vivo experiments

The *in vivo* studies were conducted under routine and approved protocols and per the Guide for the Care and Use of Laboratory Animals. A total of 2 BALB/c mice (aged 3–5 weeks) were adopted and kept under specific pathogen-free conditions. Cell suspensions (1×10^5 cells/mL) made with MCF-7 cells were subcutaneously injected into each mouse. After five days, the animals were cared for following the Guide for the Care and Use of Laboratory Animals. In the next step, the mice were intraperitoneally injected with saline

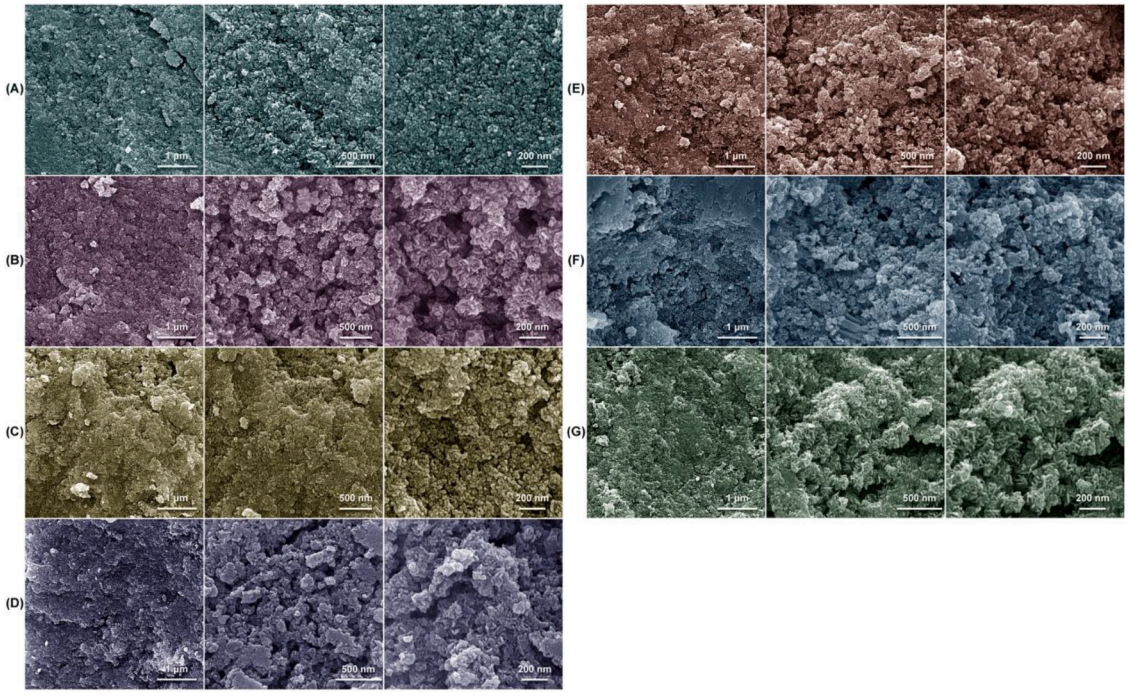

Fig. 2. FESEM images of the Zn-Cr (A), Zn-Cr/B (B), Zn-Cr/B1 (C), Zn-Cr/B2 (D), Zn-Cr/B3 (E), Zn-Cr/B4 (F) and Zn-Cr/B5 (G).

and were divided into different groups. After the injections (0.5 mL of the prepared sample), the mice were sacrificed (after two different time points of 24 and 72 h), and the breast was collected. After collecting, breast tissues were fixed in glutaraldehyde (2.5%) and osmium tetroxide (1%). To have better comparisons and images, we dehydrated the collected samples in alcohols and epoxy resin. For Histopathological evaluation, the samples were excised, and the fixation was performed in 10% formalin for one week and formalin replacement for two times, and tissues were decalcified using sulfuric acid. In the next step, samples were dehydrated in a serial dilution of ethanol, embedded in paraffin, and sectioned to 5.0 μm thicknesses using a Leica microtome (Leica Microsystems, Wetziar, Germany). Finally, Hematoxylin and Eosin (H&E) staining was performed for all sections and inspected using a light microscope (Olympus, Shinjuku, Tokyo).

3. Results and discussion

The FTIR spectra of the entire nanocomposites from each step of synthesis are shown in Fig. 1A. All of them showed a broad band at 3460 cm^{-1}, representing the different M–OH stretching modes, and at about 1630 cm^{-1}, ascribed to the hydroxyl deformation mode of

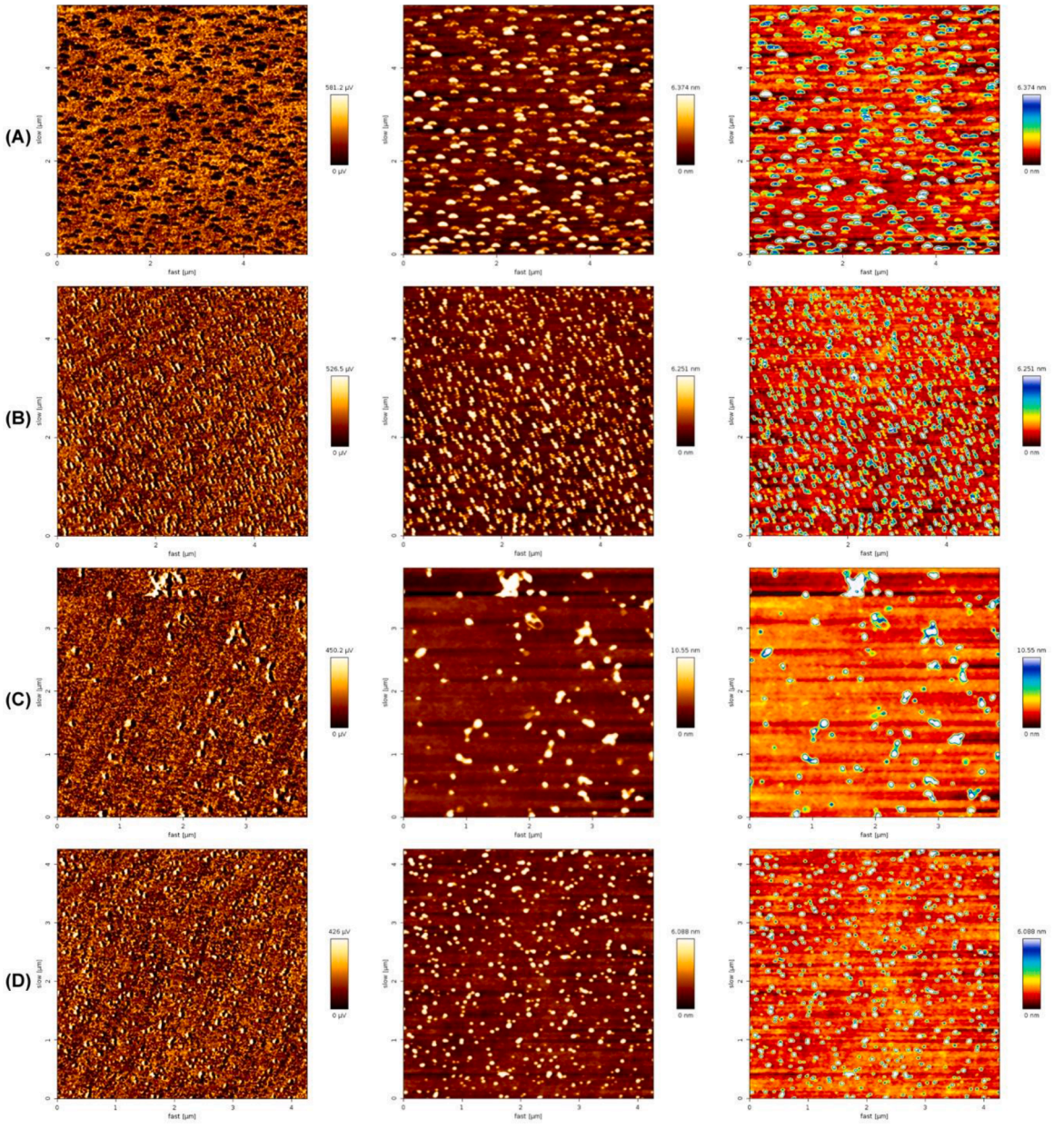

Fig. 3. AFM images of Zn-Cr (A), Zn-Cr/B (B), Zn-Cr/B1 (C), and Zn-Cr/B2 (D).

water. Two characteristic peaks at around 1380 cm^{-1} and 1506 cm^{-1} correspond to the carboxylate functional groups' symmetrical and asymmetrical stretching vibrations. A strong and broad peak at around 550 cm^{-1} represents both stretching frequencies of the LDH structure's hydroxide groups and the hydrogen bonds between them and water molecules in the interlayer structures. The IR spectrum of all synthesized nanocomposites is almost the same, indicating that the structure of LDH is preserved at all stages, and the presence of ligands and extracts on the surface of LDH does not have an effect on the IR spectrum [21,22]. Both synthesized samples of LDH have good and acceptable crystallinity, and Fig. 1C shows the PXRD pattern of ZnCr and ZnCr/B LDH. According to Fig. 1C, the diffraction peaks at around 2θ values of 11.9°, 23.5°, 29.3°, 34.3°, 38.65°, 48.3°, 59.5°, and 60.75° correspond to the crystallographic planes of (003), (006), (009), (012), (015), (018), (110) and (113) which is in good agreement with the literature [23]. According to the literature, the presence of extracts and ligands due to the presence of organic compounds in the PXRD spectrum does not make much difference [24], as observed in Fig. 1C as well. That is why the PXRD spectrum is only one of the final examples reported.

The FESEM images of the Zn/Cr-LDH are shown in Fig. 2. Fig. 2A shows that LDH has plate-like morphology and is crystallized in a hexagonal shape. Also, the size distribution is a uniform particle and below 50 μm. Fig. 2B shows the extract of *Plantago major* that is placed on top of the LDH plates. Also, in Fig. 2C-G images, the extract and the ligand between the LDH plates, according to the results published in the literature. This study showed the morphology of the synthesized LDHs that is dependent on the ratio and component of the benzamide-like ligands. Based on the literature, the functional-rich small molecules could increase the aggregations up to 62%, which is a considerably high ratio. However, one of the aims of this study is to investigate the role of aggregations in the biomedical applications of the ZnCr LDHs.

We precisely measured the thickness and roughness of the ZnCr nanosheets using atomic force microscopy (AFM), with the analysis confirming that ZnCr existed in nanosheet form with a nanosheet thickness (≈6.3 nm). Based on the results (Fig. 3), the roughness of

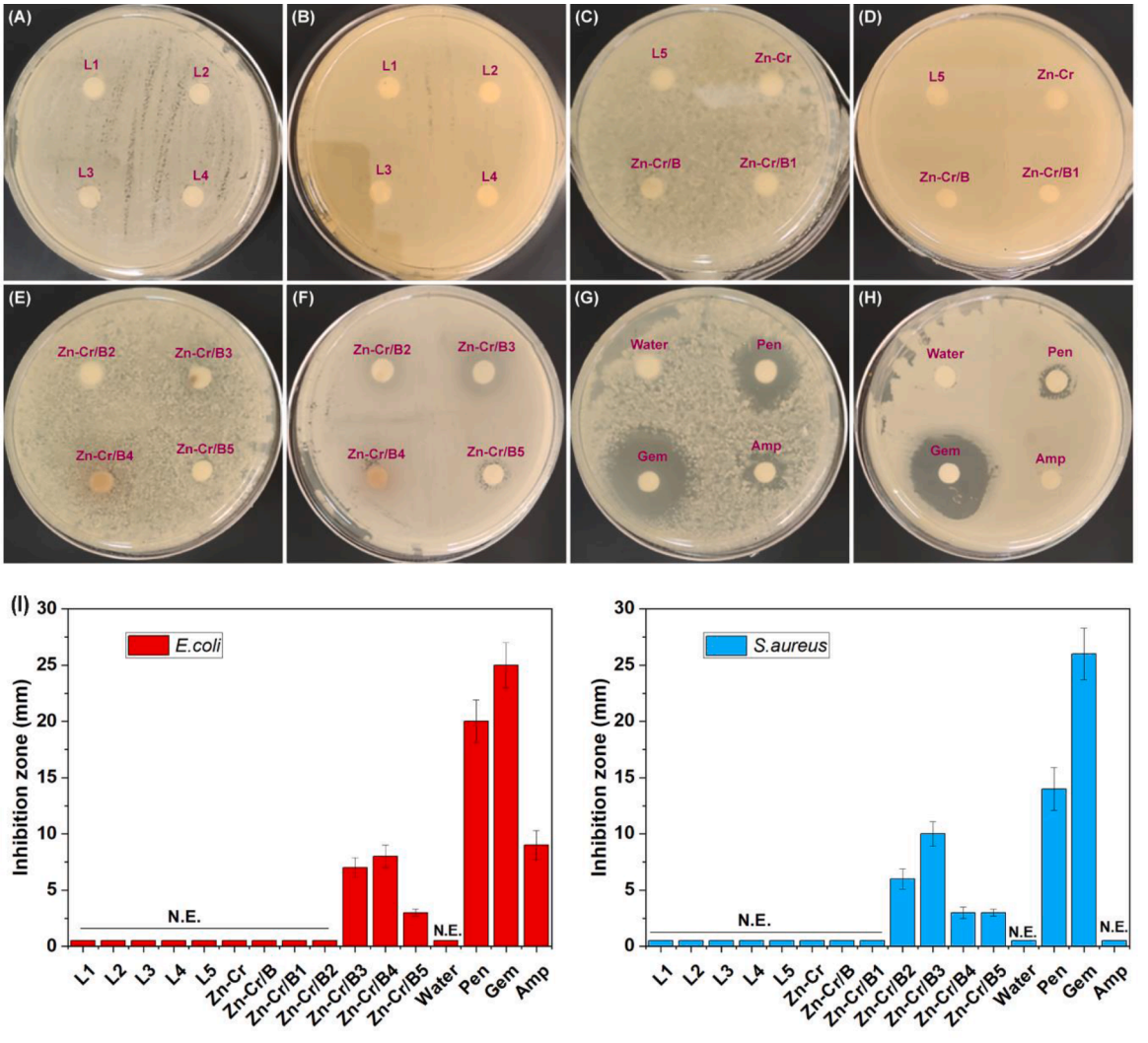

Fig. 4. The antibacterial results of synthesized compounds. A, C, E, and G represent for *E. coli* bacteria, and B, D, F, and H represent for *S. aureus* bacteria. (I) Diagram of the inhibition zone of the sample against the *E. coli S. aureus* bacteria.

the free-ligand ZnCr LDH is 10% to 29% lower than the roughness of the benzamide-like ligands decorated on the surface. Therefore, by decorating the benzamide-like molecules on the surface of the ZnCr LDHs, the roughness and the chance of physical host-guest interactions increased. Therefore, these types of molecules are also responsible for the physical host-guest interactions between the drugs and/or genes. One of the aims of this study is to investigate the role of surface roughness on biomedical performance. In this regard, by developing highly decorated nanoparticles with different surface roughness, the impact could be evaluated. Decoration of

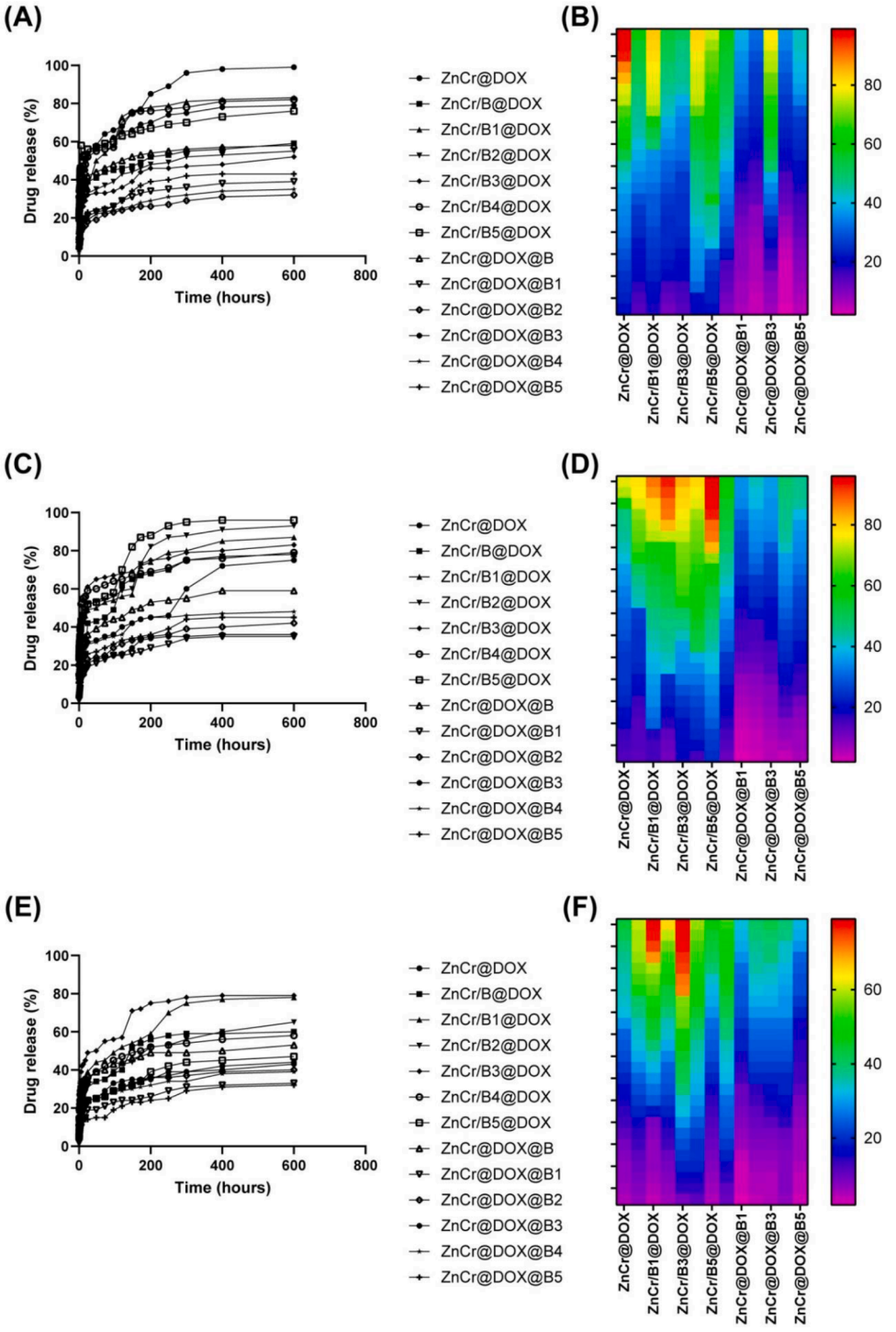

Fig. 5. Drug release profile at different pH values of (A and B) 4.5, (C and D) 5.5, and (E and F) 7.4. The normal (A, C, and E) and heat-map graphs (B, D, and F).

benzamide-like molecules on the surface of the ZnCr LDHs significantly increased the surface roughness; therefore, it is possible to increase the physical host-guest interactions between the drug and the nanostructures as well.

In this work, the antibacterial activity of the synthesized nanomaterials was investigated using the disk diffusion method *in vitro*. In this test, *E.coli* was used as a gram-negative bacterium, and *S.aureus* as a gram-positive bacterium was used. In this study, it is observed that the ligands do not have antibacterial activity, and the diameter of the killing of bacteria does not grow. Nevertheless, on the other hand, the final composition due to the structure was able to penetrate the cell wall of bacteria and destroy the bacterium and cause its death, and finally, the diameter of the killing of bacteria has grown well, which all these results can be seen in Fig. 4. The *in vitro* antibacterial activity of the synthesized nanomaterials against both the gram-negative and gram-positive bacteria is important due to the presence of oxidant agents in the physiological systems, which leads to infections and bacterium colonies. Therefore, providing a multifunctional nanomaterial that can destroy bacteria in the physiological systems could help scientists treat different diseases by using a single method.

The drug release profiles of the synthesized ZnCr LDH-based nanocarriers at pH values of 4.5, 5.5, and 7.4 were investigated to evaluate the release profile in different biological microenvironments, including cancerous cells. Before that, the drug payload was calculated by UV–vis spectroscopy and recorded by 58%. The results (Fig. 5) showed that increasing the pH value to the physiological threshold slowed the drug release to the minimum ratio. This is interesting and proves the ability to keep drugs inside the ZnCr LDH-based nanocarriers in the off-target cells/tissues. DOX is a highly toxic drug and should be maintained in off-target positions; therefore, 3D inorganic-based nanocarriers with the ability of high drug interface loading/keeping are of great importance. Interestingly, the results showed sustained and step-by-step release of the drug at any pH value by decorating the ZnCr LDH-based nanocarriers with the benzamide-like small molecules, which insists on the role of those benzamide-core molecules to eliminate the off-target interactions and increase the lifetime of the intact drug-loaded nanocarriers. Inside the body, there are lots of tissues/cells with different fluctuations of pH; therefore, maintaining the nanocarriers for a specific targeted therapy is important. For example, the designed benzamide-like decorated ZnCr LDH-based nanocarriers are desired for prostate cancer therapy especially based on their drug release profiles. Also, in case of usage for breast cancer therapy/diagnosis, the electron-rich benzamides may have considerable stability and selectivity.

Analyzing the cytocompatibility and bioavailability of the synthesized nanomaterials before any biomedical application evaluations is of great importance. In this regard, the MTT assay will usually be conducted based on cancerous and normal cells. This report conducted an MTT assay on the HEK-293, HT-29, and MCF-7 cell lines after 24 and 48 h of treatment. The results showed (Fig. 6) that the ZnCr LDH has considerable cytotoxicity in different concentrations (ranging from 1.0 to 200.0 mg/mL) in all cell lines; therefore, this inorganic nanomaterial is not a good candidate to be used as a free material. However, by decorating the surface of the ZnCr LDH with biocompatible molecules, including benzamide-like molecules, the relative cell viability increased by a ratio of between 22% to 60%. This increase in the relative cell viability proved the ability to eliminate unwanted interactions with the cell lines and target the selective tissues/cells. Also, the MTT results showed that different electronic push-pull effects of the benzamide-like molecules on the surface of the ZnCr LDH lead to different relative cell viabilities. Fast, electron-rich structures tend to interact with the cells and destroy them. Therefore, by using electron-poor ligands/linkers, the relative cell viability increased substantially.

Finally, the ability of the drug-loaded ZnCr LDH-based nanocarriers decorated with benzamide-like molecules on the cellular internalizations on the MCF-7 cell lines was evaluated. MCF-7 cell line could be considered one of the best candidates for these types of studies because of its physiological condition and also surface morphology [25]. In this manner, MCF-7 cell lines were treated with the

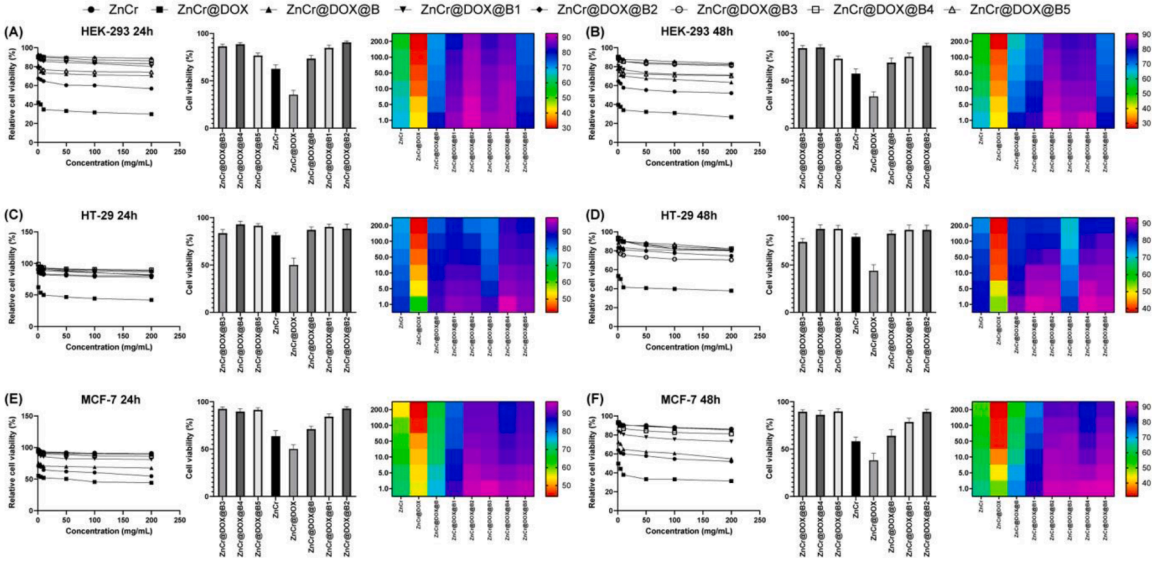

Fig. 6. MTT results on the HEK-293 (A and B), HT-29 (C and D), and MCF-7 (E and F) cell lines after 24 and 48 h of treatment.

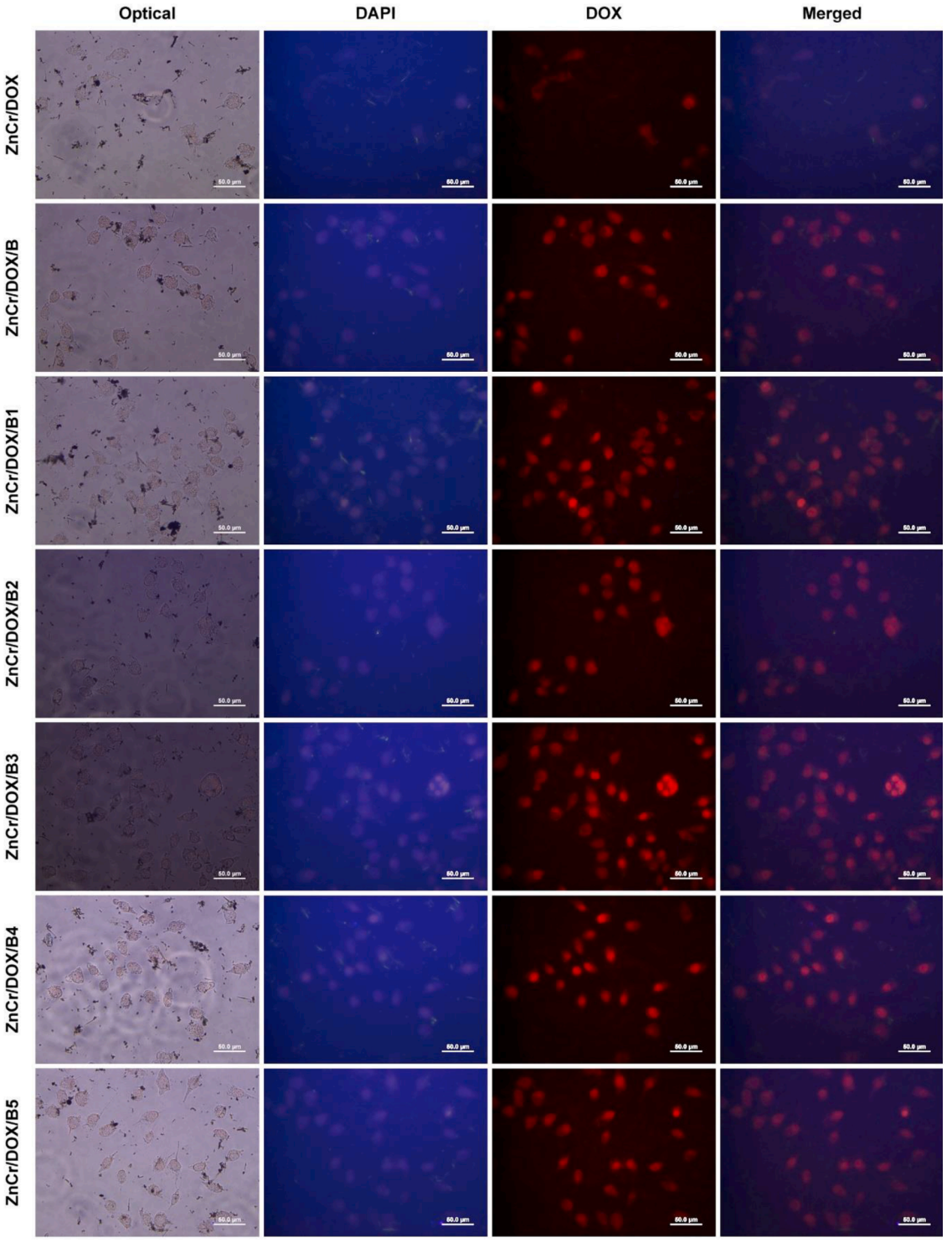

Fig. 7. 2D fluorescence images on the MCF-7 cell lines were treated after 4 h with the samples.

drug-loaded nanocarriers, and by using fluorescence microscopy, the dye contrast between the DAPI-stained cells and DOX was observed. Based on the results (Fig. 7), before coating the surface of the ZnCr LDH@DOX, the cellular populations are a small portion, which agrees with the MTT results. However, the cellular density and populations increased after decorating the surface with the benzamide-like molecules, and their morphology seemed intact. Also, by comparing the position of the DOX and DAPI, it seems that the drug is internalized to both the cell cytoplasm and nuclei. Based on the literature, to target breast cancer, both the cytoplasm and

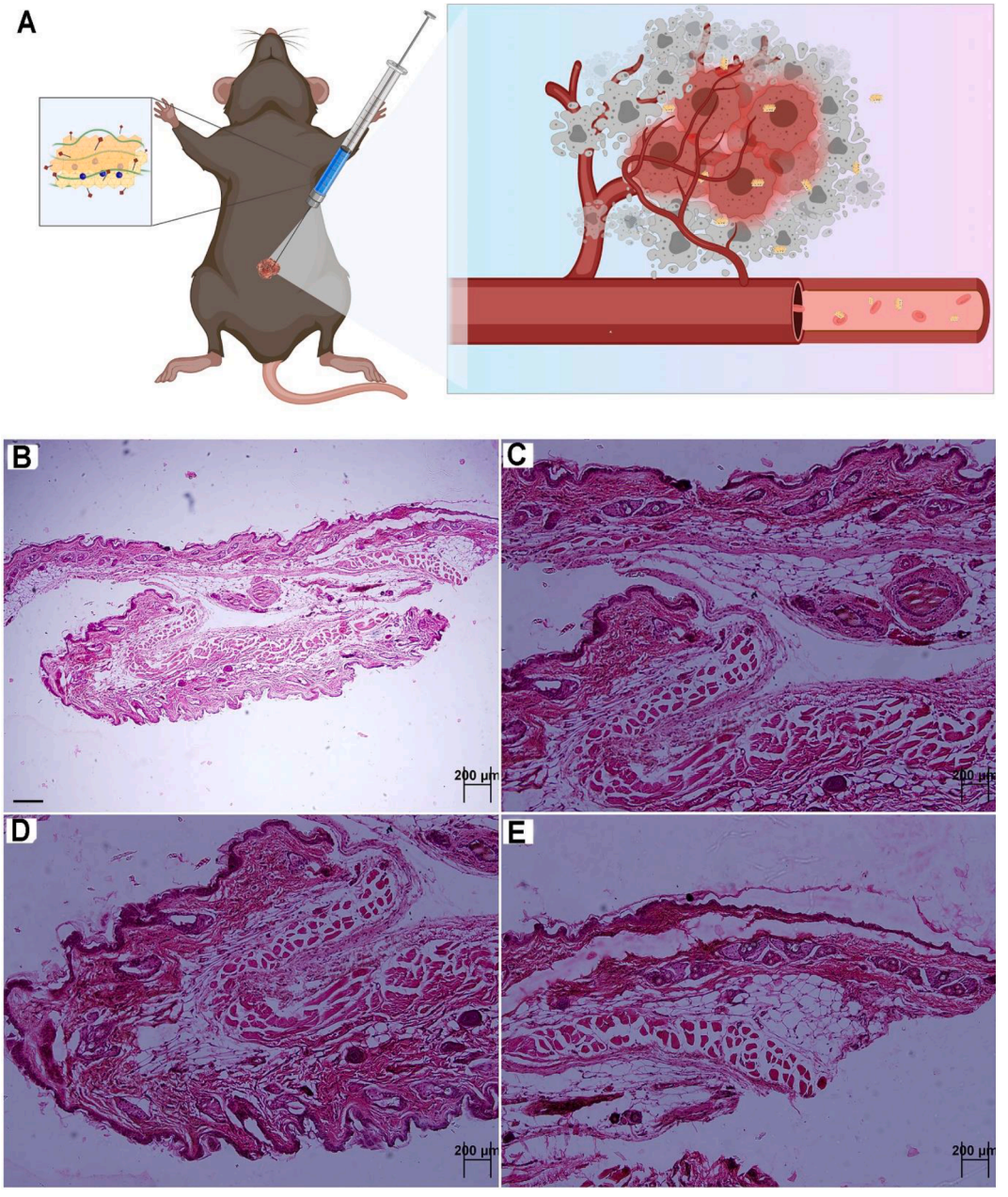

Fig. 8. H&E images of the breast cancer of the treated mice after 48 h of injections of the ZnCr LDH@DOX@B4 as the model nanocarrier for the *in vivo* experiments.

nuclei should be targeted; therefore, this inorganic nanocarrier with the ability of dual targeting is highly suggested for further studies.

In the last part, to evaluate the *in vivo* ability of the drug-loaded nanocarriers, based on the *in vitro* results, the best case, ZnCr, LDH@DOX@B4, was selected and used on the breast cancer of the treated mice. Based on the results (Fig. 8), after injection of the drug-loaded nanocarriers into the mice (with the breast cancer model), the cellular array of the breast mice did not show any abnormal aggregations/agglomerations of the nanoparticles. Also, the H&E images did not represent any abnormal and overexpressed cells/proteins/structural morphologies. Also, by comparing the results with the literature, the structure and cellular array of the breast cancer tissues with the normal cells, the treated tissue represents minor changes to the standard and normal ones in the literature. All of these results showed the ability of the best-case prepared nanocarriers to be used as the next generation of breast chemotherapy smart nanocarriers. The morphology, cellular array, and possible interactions on the surface and even below the tissue are the main points to investigate these *in vivo* results [26,27]. In this manner, a wide range of aggregations could happen on the surface of tissues and/or in the space between the cells. Our results indicate that the ZnCr LDH-based nanocarriers were not aggregated in any case, which is

considered one of the top-notch studies in the literature. Nevertheless, this phenomenon is still unknown; to this aim, more studies should be conducted on the role of different nanomaterials and/or molecules in making cellular aggregations. We know that these aggregations destroy the cellular sites differently and generate abnormal electron push-pull effects. Therefore, reducing the cellular aggregations and the surface of cells could lead to increasing biocompatibility and on-target therapeutics.

4. Conclusion

In this study, we have synthesized a new type of non-viral vector and nanocarrier based on ZnCr LDH, modified with leaf extracts and benzamide-like molecules. Those benzamide-like molecules stimulate and give the system different push-pull electronic effects. By using the electron-rich benzamide-like molecules, the relative cell viability increased up to 32%, and by using electron-poor benzamide-like molecules, the relative cell viability increased up to 29%. Also, the *in vivo* experiments on the breast cancer of the treated mice (H&E) images showed unaggregated cellular arrays. Furthermore, the antibacterial activity of the synthesized nanomaterials was evaluated on *E. coli* (gram-negative) bacterium, *S. aureus* (gram-positive) bacterium, and ZnCr LDH@B3, ZnCr LDH@B4, and ZnCr LDH@B5 showed suitable zone of inhibition (up to 10 mm), compared to the standard. Also, the *in vivo* experiments on the model mice with the MCF-7 treated breast cancers showed unaggregated cellular arrays and healthy structures. Therefore, the prepared nanocarriers and/or non-viral vectors did not change the morphology of the cells to an abnormal condition. It could be able to conclude that the benzamide-like molecules, with different push-pull electronic effects, have different biomedical performances on the antibacterial, cell viability, cellular morphology, drug release and loading; but, in most cases, all of them leads to improving the results.

Agreement

All of the authors agreed to the publication of this article on OpenNano.

CRediT authorship contribution statement

Mahsa Kiani: Methodology, Investigation, Validation. **Mojtaba Bagherzadeh:** Conceptualization, Supervision, Resources, Project administration. **Yousef Fatahi:** Validation. **Hossein Daneshgar:** Formal analysis, Validation. **Moein Safarkhani:** Writing – original draft, Investigation. **Ghazal Salehi:** Investigation, Formal analysis. **Pooyan Makvandi:** Visualization, Formal analysis. **Mohammad Reza Saeb:** Writing – review & editing. **Eder C. Lima:** Writing – review & editing. **Navid Rabiee:** Conceptualization, Supervision, Writing – review & editing.

Declaration of Competing Interests

The authors declare that they have no known competing financial interests or personal relationships that could have appeared to influence the work reported in this paper.

References

[1] H. Nosrati, et al., Prodrug polymeric nanoconjugates encapsulating gold nanoparticles for enhanced X-Ray radiation therapy in breast cancer, Adv. Healthc. Mater. 11 (3) (2022), 2102321.
[2] Z. Shokri, et al., Elucidating the impact of enzymatic modifications on the structure, properties, and applications of cellulose, chitosan, starch and their derivatives: a review, Mater. Today Chem. 24 (2022), 100780.
[3] Z. Karami, et al., Cure Index for labeling curing potential of epoxy/LDH nanocomposites: a case study on nitrate anion intercalated Ni-Al-LDH, Prog. Org. Coat. 136 (2019), 105228.
[4] Z. Karami, et al., Epoxy/layered double hydroxide (LDH) nanocomposites: synthesis, characterization, and Excellent cure feature of nitrate anion intercalated Zn-Al LDH, Prog. Org. Coat. 136 (2019), 105218.
[5] P. Higgins, S.H. Siddiqui, R. Kumar, Design of novel metal hydroxide bio-nanocomposite (CBCS@ LDH) for the scavenging of ciprofloxacin (CPN) drug from its aqueous solution: kinetic, isotherm, thermodynamic and reusability studies, Curr. Res. Green Sustainable Chem. 5 (2022), 100298.
[6] N. Rabiee, et al., ZnAl nano layered double hydroxides for dual functional CRISPR/Cas9 delivery and enhanced green fluorescence protein biosensor, Sci. Rep. 10 (1) (2020) 1–15.
[7] M. Kiani, et al., Multifunctional green synthesized Cu–Al layered double hydroxide (LDH) nanoparticles: anti-cancer and antibacterial activities, Sci. Rep. 12 (1) (2022) 1–14.
[8] H.K. Kordasht, et al., Poly (amino acids) towards sensing: recent progress and challenges, TrAC Trends Anal. Chem. 140 (2021), 116279.
[9] N. Rabiee, et al., Green porous benzamide-like nanomembranes for hazardous cations detection, separation, and concentration adjustment, J. Hazard. Mater. 423 (2022), 127130.
[10] S. Ahmadi, et al., Mission impossible for cellular internalization: when porphyrin alliance with UiO-66-NH2 MOF gives the cell lines a ride, J. Hazard. Mater. (2022), 129259.
[11] N. Rabiee, et al., Bioactive hybrid metal-organic framework (MOF)-based nanosensors for optical detection of recombinant SARS-CoV-2 spike antigen, Sci. Total Environ. 825 (2022), 153902.
[12] N. Rabiee, et al., Turning toxic nanomaterials into a safe and bioactive nanocarrier for co-delivery of DOX/pCRISPR, ACS Appl. Bio. Mater. 4 (6) (2021) 5336–5351.
[13] M.R. Saeb, et al., Green CoNi2S4/porphyrin decorated carbon-based nanocomposites for genetic materials detection, J. Bioresour. Bioprod. 6 (3) (2021) 215–222.
[14] K. Zheng, et al., Engineering crystalline CoMP-decorated (M= Mn, Fe, Ni, Cu, Zn) amorphous CoM LDH for high-rate alkaline water splitting, Chem. Eng. J. 441 (2022), 136031.
[15] G. Zhang, et al., Electron donor–acceptor effect-induced organic/inorganic nanohybrids with low energy gap for highly efficient photothermal therapy, ACS Appl. Mater. Interfaces 13 (15) (2021) 17920–17930.

[16] D. Jiang, X. Li, Q. Jia, Design of two-dimensional layered double hydroxide nanosheets embedded with Fe3O4 for highly selective enrichment and isotope labeling of phosphopeptides, ACS Sustain. Chem. Eng. 7 (1) (2018) 421–429.
[17] J. Xu, et al., Visible light-driven CO2 photocatalytic reduction by Co-porphyrin-coupled MgAl layered double-hydroxide composite, Energy Fuels 35 (19) (2021) 16134–16143.
[18] T.-.H. Kim, et al., Topology dependent modification of layered double hydroxide for therapeutic and diagnostic platform, Adv. Drug Deliv. Rev. (2022), 114459.
[19] V.A. Shirin, et al., Advanced drug delivery applications of layered double hydroxide, J. Controlled Release 330 (2021) 398–426.
[20] M. Vaishali, R. Geetha, Antibacterial activity of Orange peel oil on Streptococcus mutans and Enterococcus-An In-vitro study, Res. J. Pharm. Technol. 11 (2) (2018) 513–514.
[21] K. Parida, L. Mohapatra, Recent progress in the development of carbonate-intercalated Zn/Cr LDH as a novel photocatalyst for hydrogen evolution aimed at the utilization of solar light, Dalton Trans. 41 (4) (2012) 1173–1178.
[22] S. Mansingh, et al., Robust charge carrier engineering via plasmonic effect and conjugated Π-framework on Au loaded ZnCr-LDH/RGO photocatalyst towards H 2 and H 2 O 2 production, Inorg. Chem. Front. (2022).
[23] M. Sohail, H. Kim, T.W. Kim, Enhanced photocatalytic performance of a Ti-based metal-organic framework for hydrogen production: hybridization with ZnCr-LDH nanosheets, Sci. Rep. 9 (1) (2019) 1–11.
[24] G. Gnanasekaran, et al., Removal of hazardous material from wastewater by using metal organic framework (MOF) embedded polymeric membranes, Sep. Sci. Technol. 54 (3) (2019) 434–446.
[25] M. Akbarian, et al., Green synthesis, formulation and biological evaluation of a novel ZnO nanocarrier loaded with paclitaxel as drug delivery system on MCF-7 cell line, Colloids Surf. B 186 (2020), 110686.
[26] F. Seidi, et al., Layer-by-Layer Assembly for Surface Tethering of Thin-Hydrogel Films: Design Strategies and Applications, Wiley Online Library, 2020.
[27] Y. Zhong, et al., Natural polymer-based antimicrobial hydrogels without synthetic antibiotics as wound dressings, Biomacromolecules 21 (8) (2020) 2983–3006.